minerals

MDPI

Article

The Influence Mechanism of Magnesium Ions on the Morphology and Crystal Structure of Magnetized Anti-Scaling Products

Yubin Wang, Xinyu Mao, Wei Xiao * and Wangbo Wang

School of Resources Engineering, Xi'an University of Architecture and Technology, Xi'an 710055, China; wywywyb@xauat.edu.cn (Y.W.); mxy894749636@163.com (X.M.); wangwangbo163@163.com (W.W.)

* Correspondence: wei.xiao@xauat.edu.cn; Tel.: +86-029-82203408

Received: 14 September 2020; Accepted: 8 November 2020; Published: 10 November 2020

Abstract: Magnetization technology has been widely used in various transportation pipeline anti-scaling and descaling processes due to its simple equipment, low operating cost and low secondary pollution. To resolve structural pipeline issues in concentrations, the effects of magnesium salt concentration on conductivity, pH value and calcium ion concentration of a magnetized calcium chloride sodium bicarbonate mixed solution were studied. The results indicated that 4.0% $MgSO_4$ had the greatest anti-scaling effect under dynamic water conditions, which increased the calcium concentration of the mixed solution by 5.93%. Furthermore, the synergistic effects of 5.0% magnesium carbonate on the scaling of calcium carbonate were the largest, which reduced the calcium concentration of the mixed solution by 22.19%. Scanning electron microscope (SEM) and Raman spectra showed that magnesium carbonate reduced the effects of magnetization because it inhibited the formation of vaterite-type calcium carbonate and promoted the formation of calcite-type calcium carbonate. Magnesium sulfate can improve the anti-scaling effects of magnetization because it promotes the formation of vaterite calcium carbonate with high solubility. The results of this study can provide a theoretical basis for the scaling process and dissolution behavior regulation of calcium carbonate and have an important reference significance for scale prevention and scale removal in concentrator pipelines.

Keywords: magnetization anti-scaling; vaterite-type calcium carbonate; calcite-type calcium carbonate

1. Introduction

In the industrial production of concentrators, due to the long-term use of dynamic water rich in calcium and magnesium ions such as lime, scaling is a common occurrence in heat exchange equipment, cooling water systems and several types of transmission pipelines [1]. This type of scaling phenomenon can easily cause pipe wall corrosion, pipe blockage and slurry transportation problems, thus affecting the mineral separation process, safe operation of the concentrator and economic benefits. To ensure the efficient production of concentrators, the dynamic water system often requires descaling [2]. Therefore, for energy conservation and environmental protection purposes, it has become increasingly important to seek economic and efficient methods of scale prevention and descaling to provide technical support for normal mineral separation and index stability operations [3–5].

The water quality used in the concentrator contains Ca^{2+} and Mg^{2+}, which react with CO_2 and CO_3^{2-} in water and form inorganic salts such as $CaCO_3$; these salts are difficult to dissolve in water and gradually become sediment [6,7]. Considering the causes of scale formation, the primary methods of scale removal are mechanical, chemical reagents and high-pressure water gun sprays. These methods

have certain effects on scale prevention and removal; however, there are a few problems such as a high investment cost, a high treatment cost and secondary pollutants [6,8,9].

Several researchers have performed more detailed studies on magnetization scale prevention [10–12]. For example, Liu et al. [13] researched the synergistic scale inhibition effects of rare-earth permanent magnetic materials and polyaspartic acid and optimized this effect based on the magnetic field strength, temperature, water hardness and reagent dosage. The results indicated that magnetization treatment can enhance the scale inhibition effects of polyaspartic acid. Seung Koo et al. discussed the effects of ion and particle mechanisms of a magnetic field on the precipitation of calcium carbonate and found that the particle mechanism can reduce the concentration of calcium ions in the solution during the magnetization process whereas the ionic mechanism can reduce the formation of $CaCO_3$ crystals during the magnetization separation process [14]. Chang et al. conducted a series of growth experiments on calcium carbonate polycrystalline vaterite in a fluidized bed crystallizer subjected to a magnetic field [7]. The results indicated that under room temperature conditions, the seeds grew when they were not magnetized but they did not grow when subjected to a magnetic field. Furthermore, it was found that as the intensity of the magnetic field intensity increased, the action time decreased. Vaterite crystals grew faster in a lower pH environment whereas calcite hardly grew. Additionally, it was found that the high supersaturation and nonuniform activity ratio was beneficial to vaterite growth.

Consequently, a few scholars have also explored the practical application of magnetization scale prevention. Wang et al. designed a dynamic electromagnetic test device [15]. By analyzing and comparing the characteristics of conductivity over time, the metastable curves of calcium carbonate crystals under different influencing factors (such as solution concentration and electromagnetic field strength) were obtained. Deng et al. researched the effects of an adjustable constant magnetic field with a maximum flux density of 4100 MT on the precipitation process of calcium carbonate in hard water without impurity ions [16]. The results indicated that the magnetic field changed the dehydration process of $CaCO_3$ as the precursor of a crystal nucleus by affecting the hydration process of ions in the solution, which then changed the structure of the water mass and affected the precipitation process of $CaCO_3$.

To solve the above-mentioned problems, new and efficient scale prevention and removal technologies such as magnetization scale prevention and scale removal technology have gradually attracted the attention of researchers [10,17,18]. The primary advantage of this technology is that there is no secondary pollution of chemical agents and the application range is wide [19]. In addition, the magnesium ions and calcium ions in the water are elements of the same main group, which will also have a certain impact on the crystallization process of calcium carbonate in the pulp. However, there are certain problems in this process such as ideal laboratory indexes and unstable industrial application effects. Additionally, the adaptability of the process to different industries varies. Thus, using anti-scaling and descaling of the pipeline in the concentrator as the breakthrough point, the variation law of the solubility of magnetized calcium carbonate is characterized by the detection methods of conductivity, pH value and calcium ion concentration. This study can not only provide a theoretical basis for scale prevention and descaling of slurry pipelines in concentrators but also offer a reference for the application of magnetization technology in different fields.

2. Materials and Methods

2.1. Materials and Reagents

Ultra-pure water with a conductivity of 18.2 MΩ·cm was obtained from a USF-ELGA Maxima water purification system (MEDICA 60, ELGA Company, Buckinghamshire, UK). All of the reagents in this study were of analytical purity grade.

2.2. Methods

2.2.1. Anti-Scaling Tests Using a Parallel Magnetic Field

The design of the parallel magnetic field anti-scaling test system is shown in Figure 1. The magnetic field parameters used were as follows: a 9 mm diameter coil was wound into 100 turns and then a square wave with a current frequency of 0.6 kHz was magnetized for 0.5 h. Figure 1a illustrates the anti-scaling test process while Figure 1b,c provide schematic diagrams of the magnetization anti-scaling test system under a vertical flow magnetic field for static and dynamic water conditions, respectively. During the test, a specific number of turns of copper enameled wire was wound on the outer wall of a 1000 mL beaker and a signal generator was connected for the magnetization treatment. It should be noted that the magnetic field was parallel to the pipeline during the test.

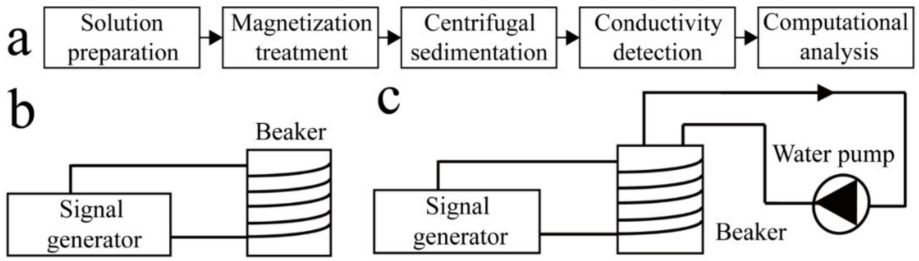

Figure 1. A schematic diagram of a parallel magnetic field anti-scaling test system. (**a**) Magnetization anti-scaling test process; (**b**) Static water condition; (**c**) Dynamic water condition.

Calcium chloride (1000 mg/L) and sodium bicarbonate with a molar ratio of 1:1 were weighed and dissolved in 1000 mL of ultra-pure water to prepare a mixed solution. The mixed solution was magnetized with different magnesium salts, static water and dynamic water (flow rate of 900 mL/min) for 30 min. After the magnetization treatment, 50 mL of supernatant were taken using a pipette to detect the pH value, conductivity and calcium ion concentration. Finally, the solution was filtered and dried for SEM and Raman spectroscopy.

2.2.2. Solution pH Detection

The primary principle of the pH value detection of the solution was to determine the pH value of the solution by measuring the electrode potential of a selective indicator electrode, which had a reversible reaction to hydrogen ions in the solution and changed regularly with the pH value [20]. Fifty milliliters of a supernatant water sample from the magnetization scale removal test were taken. The pH value of the solution was detected five times and the average value was recorded as the final test result.

2.2.3. Solution Conductivity Detection

The primary principle of the conductivity meter measurement method was to use the conductive effect generated by the movement of the charged ions in an electrolyte solution under the effects of an electric field. According to a previous study [21], when the calcium carbonate precipitation dissolves, the conductivity and concentration of the calcium ions and carbonate ions in the solution increases; thus, a change in the ion concentration in the solution can be reflected by the conductivity. The detection steps were as follow. We obtained a 50 mL water sample for the magnetization and descaling test. This was placed in a centrifuge at 2800 rpm for 20 min in a low-speed centrifuge. An appropriate amount of supernatant was added and conductivity was detected by using a conductivity meter five times. The average value as the final test result was then calculated.

2.2.4. Calcium Ion Concentration Detection

Common methods for detecting calcium ion concentration include the atomic absorption and complexometric titration methods. Fifty milliliters of the supernatant were taken from the magnetization solution and 2 mL of sodium hydroxide with a concentration of 2 mol/L and 0.2 g of ammonium purpurea indicator were added. During the titration process, the conical flask was shaken continuously and an appropriate amount of EDTA (ethylene diamine tetraacetic acid) solution with a concentration of 10 mmol/L was added until the solution changed from a purplish red to a bright blue color. The volume of the EDTA solution consumed was then recorded and the average value of five titrations was used as the final test result.

2.2.5. Scanning Electron Microscopy

Scanning electron microscopy is a detection method that uses an incident electron as an excitation source to scan the surface of a sample and analyze the morphology and composition of the surface of the material. The working parameters of the quanta 200 scanning electron microscope (Quanta200, FEI Company, Hillsboro, OR, USA) used in the test were as follows: accelerating voltage 15 kV, magnification 5000, 10,000 and 15,000. The sample preparation method was as follows. The dried powder sample was evenly coated on the conductive adhesive, the crystal morphology was observed by scanning electron microscope after spraying gold and the element types and relative atomic content on the sample surface were analyzed by EDS.

2.2.6. Raman Spectra Analysis

The normal vibration frequency and related vibration energy levels of the molecules were studied by an inVia reflex micro confocal laser Raman spectrometer (inVia-Reflex, Renishaw, Wotton-under-Edge, UK) and the molecular structure, functional groups and crystal types of the samples were obtained. The operating parameters of inVia reflex micro confocal laser Raman spectrometer were as follows: spectral resolution ≤2 cm^{-1}; spatial resolution: 1 μm in a transverse direction and 2 μm in a longitudinal direction; laser wavelength was 532 nm; scanning range was 100–1400 cm^{-1}; the minimum step size was 0.1 μm; repeatability was 0.2 μm.

3. Results and Discussion

3.1. Effects of Mg^{2+} Ions on the pH of the Solution

The effects of different magnesium salt hydrolyses on the solution's pH value were studied in both static and flowing water and the results are shown in Figure 2.

When magnetized ultra-pure water was used as a solvent, the magnesium carbonate was weakly alkaline and the magnesium sulfate was weakly acidic so the pH value of the $MgCO_3$ solution increased with an increase in the $MgCO_3$ concentration whereas the $MgSO_4$ solution decreased with an increase in the $MgSO_4$ concentration (Figure 2a). In static water, the pH value of the $MgCO_3$ solution first increased rapidly at a low concentration then increased slowly and eventually stabilized at approximately 10.1. In flowing water, the increasing trend of the pH value of the $MgCO_3$ solution was faster than in static water. When the concentration of $MgCO_3$ was high (4% and 5%), the pH value of the $MgCO_3$ solution was stable at approximately 10.0 in both static and flowing water. In the $MgSO_4$ solution, the pH value of the $MgSO_4$ solution decreased slowly with an increase in concentration regardless of whether it was static or flowing water. It should be noted that the decrease between the pH values was consistent; i.e., the pH value in static water was always approximately 0.6 higher than that in flowing water.

However, in the magnetized $CaCl_2$-$NaHCO_3$ mixed solution, the hydrolysis of magnesium salts had minimal effects on the pH value of the solution (Figure 2b). With an increase in the magnesium salt concentration, the pH value of the solution in static water was stable between 7.0–7.1. The pH value of flowing water was slightly higher than that of static water, which was stable at approximately

7.4. This phenomenon indicated that $CaCl_2$-$NaHCO_3$ acts as an extremely suitable buffer for the pH of the solution. One likely reason was that the anions in the added magnesium salts reacted with the calcium ions in the solution to form the insoluble precipitate.

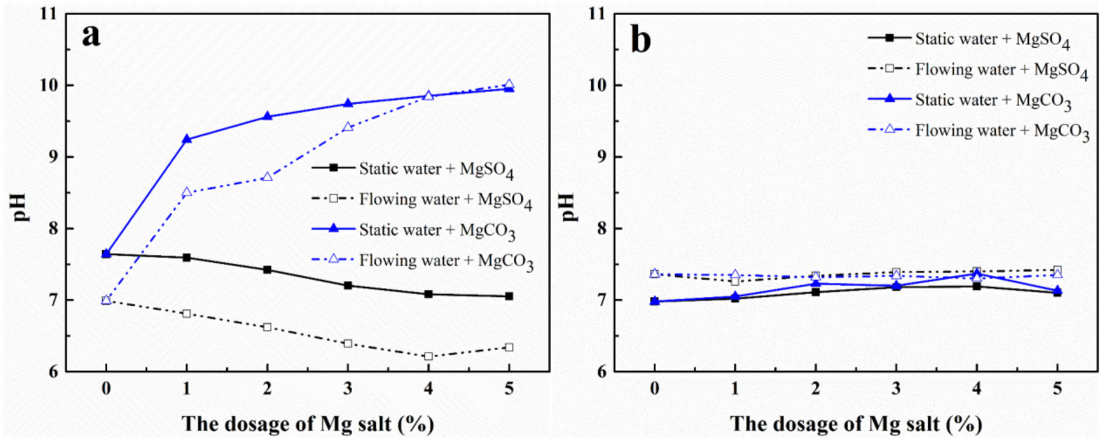

Figure 2. The relationship between the pH value of magnetized distilled water (**a**) and magnetized calcium chloride sodium bicarbonate solution (**b**) with magnesium salt concentration under different water flow conditions.

3.2. Effects of Mg^{2+} Ions on the Conductivity of the Solution

The relationship between the conductivity of the solution and the concentration of magnesium salts was investigated for both static and flowing water and the results are shown in Figure 3.

In magnetized ultra-pure water, the conductivity of the solution had a good linear correlation with the concentration of the magnesium salts (Figure 3a). The conductivity of the $MgSO_4$ solution in the dynamic water flow was higher than that in the static water flow whereas the conductivity of the $MgCO_3$ solution had a minor relationship with the flow state. At the same concentration, the conductivity of the $MgSO_4$ solution was higher than that of the $MgCO_3$ solution. It is possible that the solubility of $MgSO_4$ was higher than that of $MgCO_3$, which led to the high concentration of magnesium ions in the solution and good conductivity.

In the magnetized $CaCl_2$-$NaHCO_3$ mixed solution, the effects of $MgCO_3$ and $MgSO_4$ on the conductivity of the solution were different (Figure 3b). In static water, the conductivity of the $MgCO_3$ solution first increased and then decreased slowly with an increase in the $MgCO_3$ concentration whereas the conductivity of the $MgSO_4$ solution had opposing results. When the concentration of $MgCO_3$ was 1%, the static water solution reached its maximum conductivity (2853 $\mu S \cdot cm^{-1}$). When the concentration of $MgSO_4$ was 3%, the minimum conductivity (2681 $\mu S \cdot cm^{-1}$) of the static aqueous solution was obtained.

In the dynamic flow, when the concentration of $MgCO_3$ was between 2–4%, the conductivity of the solution first increased and then decreased. When the concentration of $MgCO_3$ was less than 2 or greater than 4, the conductivity of the solution remained unchanged. However, the conductivity of the $MgSO_4$ solution increased with an increase in the concentration in flowing water. When the concentration of $MgSO_4$ was 4%, the conductivity of the solution reached its maximum value (2937 $\mu S \cdot cm^{-1}$). As the conductivity of the inorganic salt solution was positively correlated with the concentration of charged ions in the solution, as the conductivity increased, the concentration of Ca^{2+} ions in the solution increased. Therefore, $MgSO_4$ could promote the dissolution of magnetized $CaCO_3$ more effectively than $MgCO_3$.

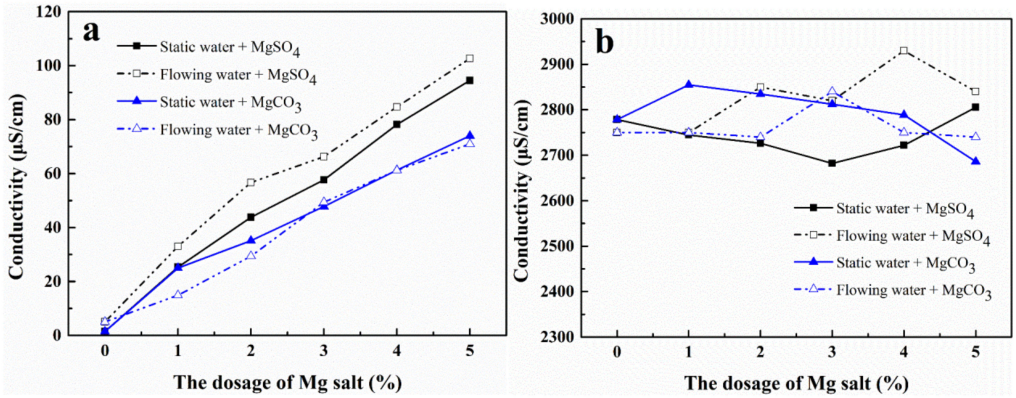

Figure 3. The effects of the concentration of magnesium salts on the conductivity of the solution for both static and flowing water. (**a**) magnetized distilled water;(**b**) magnetized calcium chloride sodium bicarbonate solution;

3.3. Effects of Mg^{2+} Ions on the Ca^{2+} Concentration of the Solution

The effects of the magnesium salts on the concentration of Ca^{2+} ions in the magnetized $CaCl_2$-$NaHCO_3$ mixed solution is shown in Figure 4 for both static and flowing water.

In static water, the concentration of Ca^{2+} ions decreased with an increase in the $MgCO_3$ concentration whereas it first decreased and then increased with an increase in the $MgSO_4$ concentration (Figure 3a). With an increase in the $MgCO_3$ concentration, the Ca^{2+} ion concentration of the solution decreased from 239.74 mg·L^{-1} to 220.19 mg·L^{-1}. With an increase in the $MgSO_4$ concentration, the concentration of the Ca^{2+} ions in the solution first decreased and then increased. When the concentration of $MgSO_4$ was 3.0%, the minimum concentration of the Ca^{2+} ions in the solution was 219.62 mg·L^{-1}.

In flowing water, the concentration of the Ca^{2+} ions in the solution increased with an increase in the $MgSO_4$ concentration. When the concentration of $MgSO_4$ was 4.0%, the maximum concentration of the Ca^{2+} ions in the solution was 240.38 mg·L^{-1}, which indicated an increase of 5.93%. However, with an increase in the $MgCO_3$ concentration, the concentration of the Ca^{2+} ions in the solution first increased and then decreased. When the concentration of $MgCO_3$ was more than 3.0%, the concentration of the Ca^{2+} ions in the solution decreased significantly. When the concentration of $MgCO_3$ was 5.0%, the minimum concentration of the Ca^{2+} ions in the solution was 207.69 mg·L^{-1}, which indicated a decrease of 22.19%. As the solubility of magnesium carbonate in water is greater than that of calcium carbonate, magnesium carbonate will hinder the dissolution of calcium carbonate and reduce the calcium ion concentration.

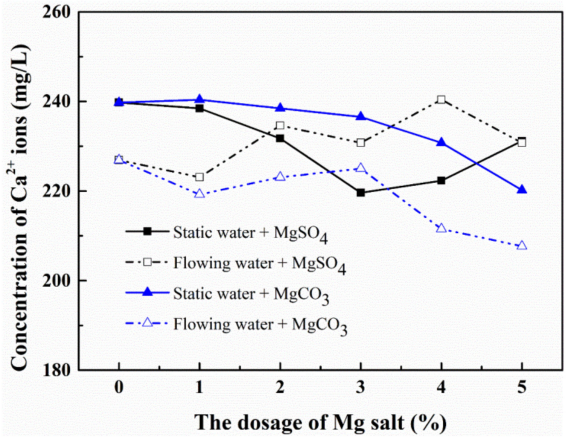

Figure 4. The effects of magnesium salts on the concentration of Ca^{2+} ions in the magnetized $CaCl_2$-$NaHCO_3$ mixed solution.

3.4. Morphology Analysis of Magnesium Sulfate for Magnetization Anti-Scaling Products

According to the above experimental results, magnesium sulfate can promote the dissolution of calcium carbonate. Figure 5 shows the morphology changes of different concentrations of the magnesium sulfate solution on the dissolution behavior of calcium carbonate after magnetization.

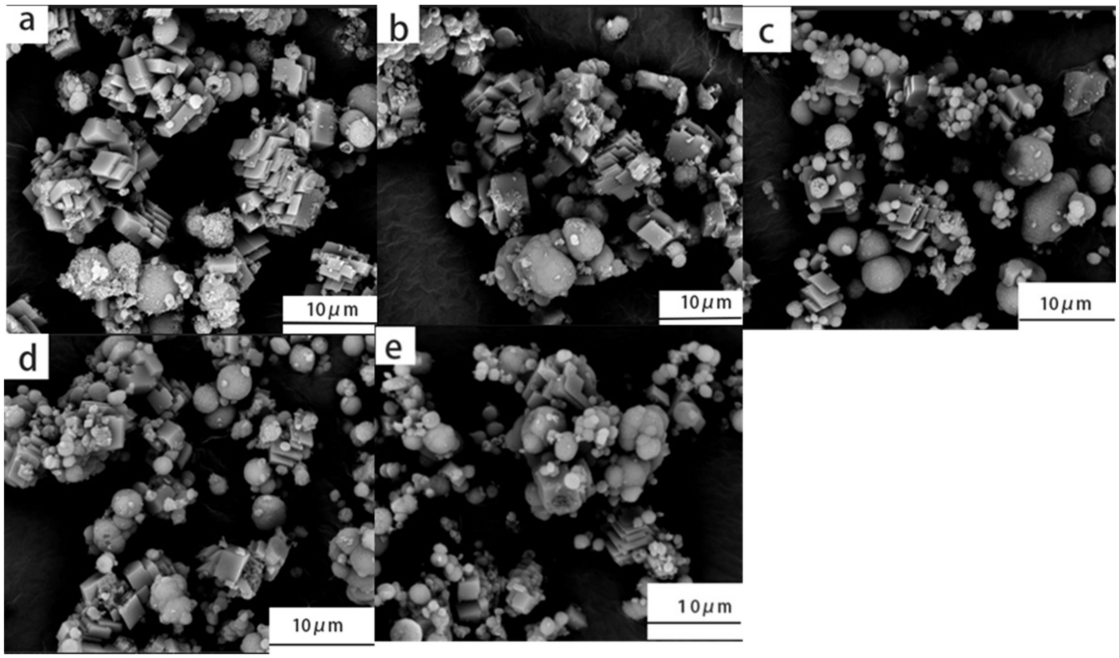

Figure 5. The effects of magnesium sulfate dosage on the morphology of magnetized anti-scaling products: (**a**) 1%; (**b**) 2%; (**c**) 3%; (**d**) 4%; (**e**) 5%.

With an increase in the magnesium sulfate concentration, the precipitate of calcium carbonate in the solution gradually transformed from cubic to spherical. The content of calcium carbonate precipitation in the solution decreased gradually. This phenomenon was consistent with that reported in the literature [22]; i.e., magnesium sulfate can promote the dissolution of cubic calcium carbonate under magnetization conditions and form a vaterite such as calcium carbonate. With an increase in the magnesium sulfate concentration, the vaterite-type calcium carbonate content increased gradually. When the concentration of magnesium sulfate was 5.0%, the size of the cubic calcite calcium carbonate increased and a few crystal defects appeared. Simultaneously, the agglomeration of vaterite-type calcium carbonate was more significant. Therefore, the appropriate amount of magnesium sulfate can promote the formation of vaterite-type calcium carbonate with high solubility, prevent its agglomeration and improve the magnetization anti-scaling effects under flowing water conditions.

3.5. Material Composition Analysis of Magnesium Sulfate for Magnetization Anti-Scaling Products

Based on the analysis of the morphology of magnetized anti-scaling products when subjected to magnesium sulfate, the effects of magnesium sulfate on the chemical structure of calcium carbonate precipitation were studied using Raman spectroscopy. The results are shown in Figure 6.

Before and after adding magnesium sulfate, the Raman shift peak appeared at 1080–1090 cm^{-1} (Figure 6). Based on the standard spectrum, the standard Raman shift peak corresponding to the calcite-type calcium carbonate was 1086 cm^{-1} whereas that of vaterite was 1089 cm^{-1}. To further analyze the crystal structure and the content of calcium carbonate in the precipitation particles, we conducted a thorough analysis of the Raman spectrum and the results are shown in Figure 6b–f and Table 1.

In the fitting peaks in Figure 6b–f, only two Raman characteristic shift peaks of calcite and vaterite were found and the integral area of these two peaks changed with an increase in the magnesium sulfate concentration.

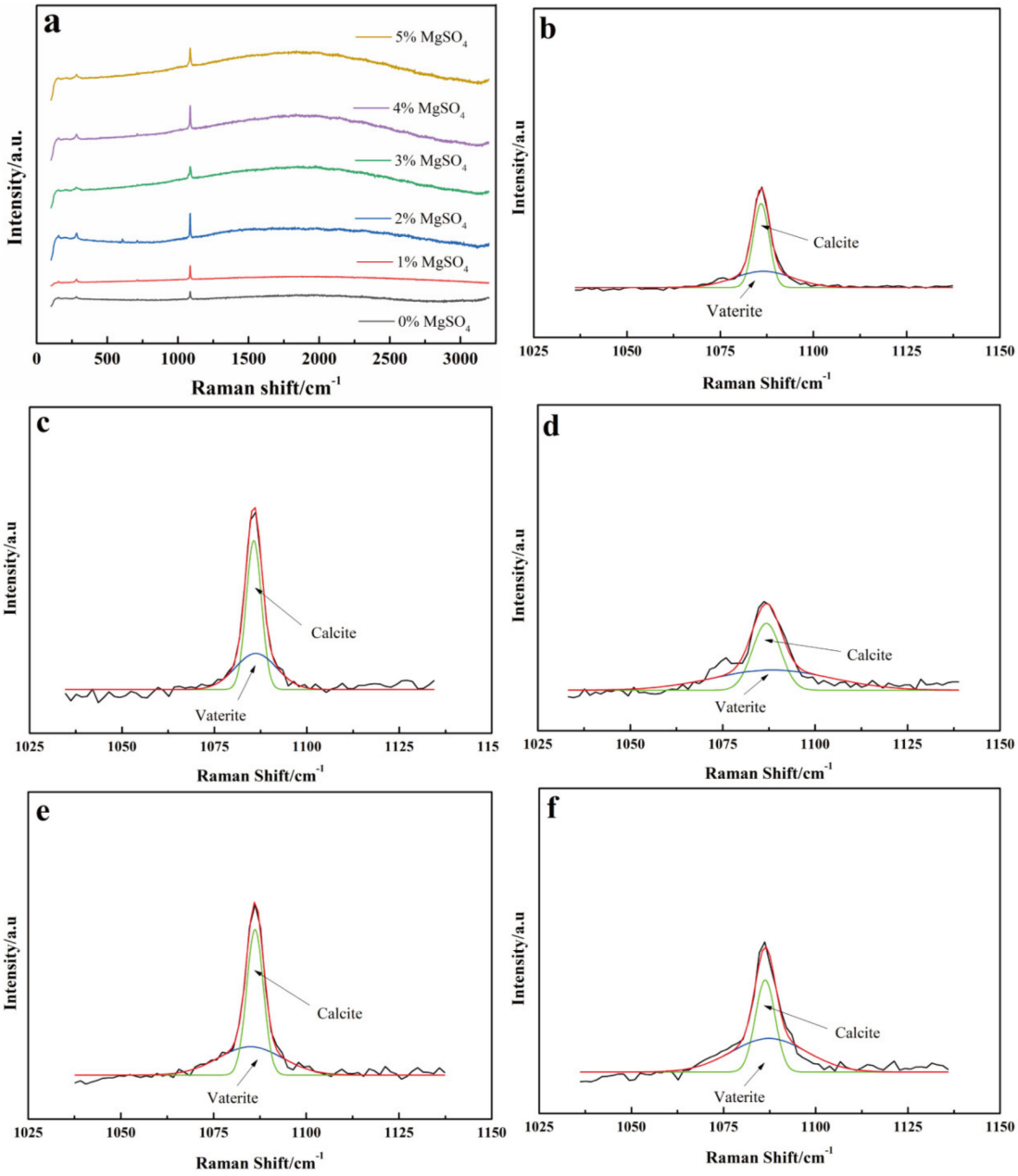

Figure 6. A full spectrum and thorough analysis of magnetized anti-scaling products with different magnesium sulfate dosage: (**a**) full spectrum; (**b**) 1%; (**c**) 2%; (**d**) 3%; (**e**) 4%; (**f**) 5%.

With an increase in the magnesium sulfate content, the total peak area of calcium carbonate increased gradually (Table 1). The calcite-type calcium carbonate content, which hindered the anti-scaling effect, gradually decreased whereas the vaterite-type calcium carbonate content, which promoted the anti-scaling effect, gradually increased. When the concentration of magnesium sulfate was 5.0%, the vaterite-type calcium carbonate content was higher than the calcite-type calcium carbonate content; however, the agglomeration phenomenon was more significant and the size of the calcite-type calcium carbonate product was higher. These phenomena not only affected its solubility in

water but also made it easier to deposit scales. The magnetization anti-scaling effect was optimal when the concentration of magnesium sulfate was 4.0%.

Table 1. The relationship between the content of the different crystal forms of calcium carbonate and the amount of magnesium sulfate in the magnetized anti-scaling samples.

Magnesium Sulfate/%	Calcite Peak Area	Vaterite Peak Area	Total Peak Area	Calcite Content/%	Vaterite Content/%
1.0	28,750	20,500	49,250	58.38	41.62
2.0	45,918	33,220	79,139	58.02	41.98
3.0	41,043	52,202	93,246	44.02	55.98
4.0	39,584	52,662	92,246	42.91	57.09
5.0	39,991	55,565	95,557	41.85	58.15

3.6. Morphology Analysis of Magnesium Carbonate for Magnetization Anti-Scaling Products

Figure 7 illustrates the relationship between the morphology of calcium carbonate and the amount of magnesium carbonate.

As shown in Figure 7a,b, combined with the effects of magnesium carbonate on the solubility of calcium carbonate, the inhibition effect of magnesium carbonate could reduce the number of calcium ions in the solution, which was not conducive to the formation of vaterite-type calcium carbonate. Furthermore, it can be seen from Figure 7c–e that with an increase in the magnesium carbonate mass fraction, the proportion of cubic calcite-type calcium carbonate increased gradually whereas the proportion of vaterite-type calcium carbonate decreased gradually. When the mass fraction of magnesium carbonate was 5.0%, the vaterite-type calcium carbonate was scarce in the magnetized anti-scaling products and the calcite-type calcium carbonate crystal surface was smooth with minimal defects. Magnesium carbonate promoted the formation of calcite-type calcium carbonate with low solubility; i.e., magnesium carbonate was not conducive to improving the magnetization anti-scaling effect under dynamic water conditions. When the mass fraction of magnesium carbonate was 5.0%, the synergistic effects of the calcium carbonate scale were the strongest.

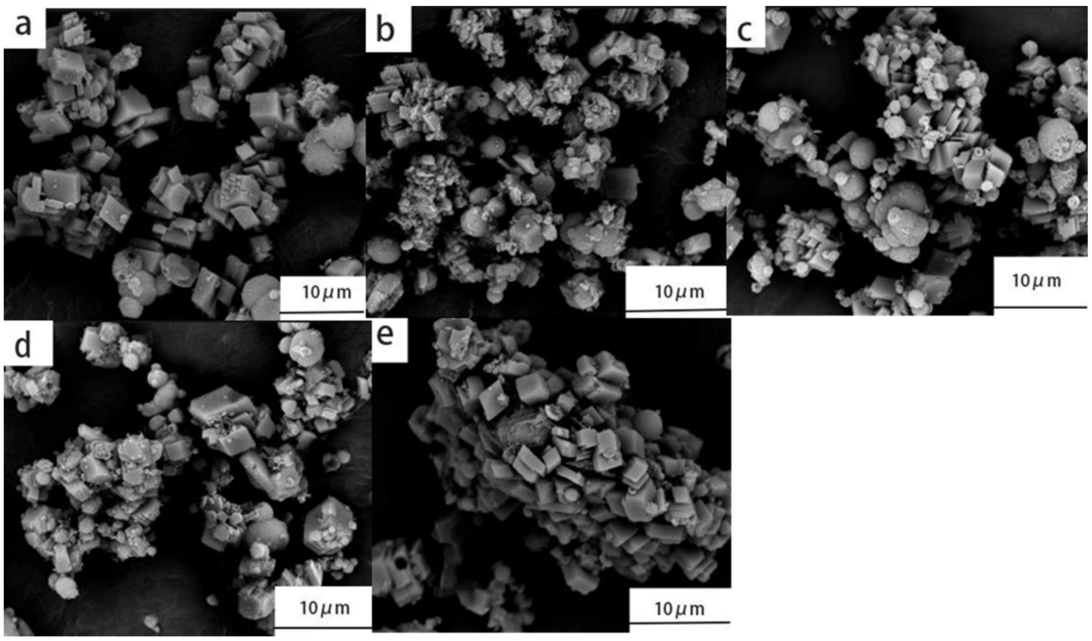

Figure 7. The effects of magnesium carbonate dosage on the morphology of magnetized anti-scaling products: (**a**) 1%; (**b**) 2%; (**c**) 3%; (**d**) 4%; (**e**) 5%.

3.7. Material Composition Analysis of Magnesium Carbonate for Magnetization Anti-Scaling Products

To further study the effect of magnesium carbonate on the structure of magnetized anti-scaling products, Raman spectroscopy was used to detect and analyze the magnetized anti-scaling products. The results are shown in Figure 8 and Table 2.

It can be seen from Figure 8 that the magnetized anti-scaling products after the addition of magnesium carbonate were a mixture of calcite and vaterite. With an increase in the magnesium carbonate concentration, the proportion of the calcite-type calcium carbonate increased gradually. When the mass fraction of magnesium carbonate was 5.0%, the calcite-type calcium carbonate content reached 79.27%, which was considerably higher than the vaterite-type calcium carbonate content. As the vaterite-type calcium carbonate can promote dissolution of the scale, it was necessary to create conditions in the solution to achieve the highest possible vaterite-type calcium carbonate content. Therefore, as the concentration of magnesium carbonate in the solution increased, the magnetization and scale prevention became less favorable.

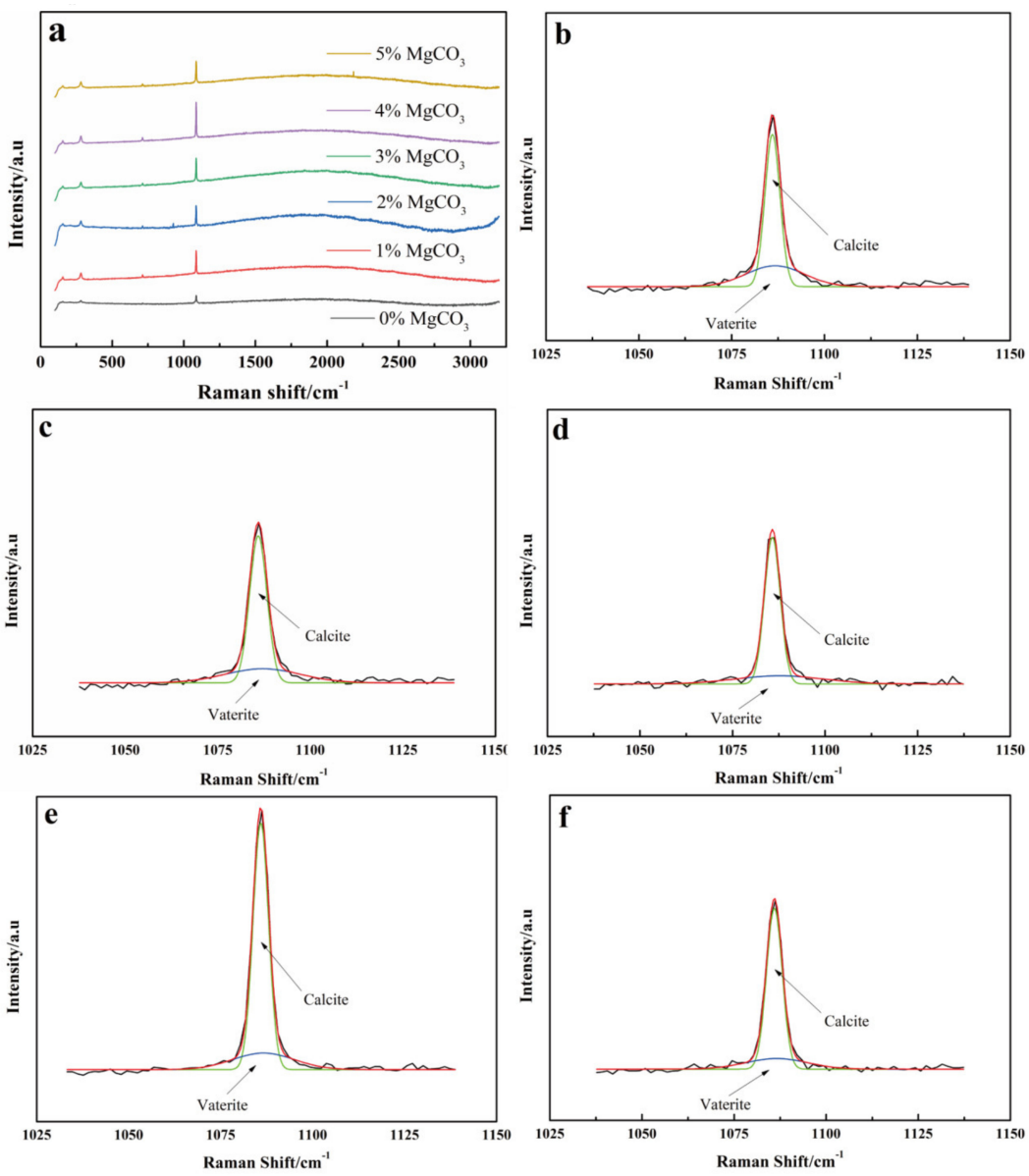

Figure 8. A full spectrum and thorough analysis of the magnetized anti-scaling products with different magnesium carbonate dosage: (**a**) full spectrum; (**b**) 1%; (**c**) 2%; (**d**) 3%; (**e**) 4%; (**f**) 5%.

Table 2. The relationship between the content of the different crystal forms of calcium carbonate and the amount of magnesium carbonate in magnetized anti-scaling samples.

Magnesium Carbonate/%	Calcite Peak Area	Vaterite Peak Area	Total Peak Area	Calcite Content/%	Vaterite Content/%
1.0	49,386	26,269	75,656	65.28%	34.72%
2.0	55,476	23,099	78,576	70.60%	29.40%
3.0	50,368	15,922	66,290	75.98%	24.02%
4.0	84,429	22,610	107,039	78.88%	21.12%
5.0	55,612	14,541	70,154	79.27%	20.73%

4. Conclusions

(1) Under dynamic water conditions, 4.0% $MgSO_4$ had the greatest anti-scaling effect, which could increase the calcium ion concentration of the calcium chloride sodium bicarbonate solution by 5.93%. However, the synergistic effects of 5.0% magnesium carbonate on calcium carbonate scaling were the strongest, which could reduce the calcium ion concentration of the calcium chloride sodium bicarbonate solution by 22.19%.

(2) Magnesium carbonate reduced the effects of magnetization because it inhibited the formation of vaterite-type calcium carbonate and promoted the formation of calcite-type calcium carbonate crystals. Magnesium sulfate can improve the effects of magnetization because magnesium sulfate promoted the formation of vaterite calcium carbonate with a high solubility.

Author Contributions: Y.W. and W.X. conceived of and designed the experiments; W.W. prepared the samples and performed the experiments; Y.W. and X.M. analyzed the data and Y.W., W.W., W.X. and X.M. contributed to the writing and revising of the paper. All authors have read and agreed to the published version of the manuscript.

Funding: This research was funded by the National Natural Science Foundation of China (No. 51971218).

Conflicts of Interest: The authors declare no conflict of interest.

References

1. Yan, M.; Tan, Q.; Liu, Z.; Li, H.; Zheng, Y.; Zhang, L.; Liu, Z. Synthesis and application of a phosphorous-free and non-Nitrogen polymer as an environmentally friendly scale inhibition and dispersion agent in simulated cooling water systems. *ACS Omega* **2020**, *5*, 15487–15494. [CrossRef] [PubMed]
2. Coppola, A.; Montagnaro, F.; Scala, F.; Salatino, P. Impact fragmentation of limestone-based sorbents for calcium looping: The effect of steam and sulphur dioxide. *Fuel Process. Technol.* **2020**, *208*, 106499. [CrossRef]
3. Georgiou, D.; Bendos, D.; Kalis, M.; Koutis, C. Removal and/or prevention of limescale in plumbing tubes by a radio-frequency alternating electric field inductance device. *J. Water Process Eng.* **2018**, *22*, 34–40. [CrossRef]
4. Sternisa, M.; Mraz, J.; Mozina, S.S. Microbiological aspects of common carp (Cyprinus carpio) and its processing-relevance for final product quality: A review. *Aquac. Int.* **2016**, *24*, 1569–1590. [CrossRef]
5. Sohn, C.-H.; Gu, S.M.; Kim, C.S.; Kim, G.U. Prevention of Particulate Scale with a New winding Method in the Electronic Descaling Technology. *Trans. KSME B* **2002**, *26*, 658–665. [CrossRef]
6. Agnihotri, B.; Sharma, A.; Gupta, A.B. Characterization and analysis of inorganic foulants in RO membranes for groundwater treatment. *Desalination* **2020**, *491*, 114567. [CrossRef]
7. Chang, M.C.; Tai, C.Y. Effect of the magnetic field on the growth rate of aragonite and the precipitation of $CaCO_3$. *Chem. Eng. J.* **2010**, *164*, 1–9. [CrossRef]
8. Tamura, Y.; Ueoka, S.; Kimura, Y.; Kabeya, K. Influence of injection distance on water droplet behavior in high pressure descaling. *ISIJ Int.* **2020**, *60*, 128–135. [CrossRef]
9. Garcia, D.; Bruyere, V.I.E.; Bordoni, R.; Olmedo, A.M.; Morando, P.J. Malonic acid: A potential reagent in decontamination processes for Ni-rich alloy surfaces. *J. Nucl. Mater.* **2011**, *412*, 72–81. [CrossRef]
10. Meng, X.; Du, J.; Li, K.; Zhang, Z.; He, W.; Liu, Z. Research on magnetization and scale inhibition technology of China oilfield wastewater. *Fresenius Environ. Bull.* **2019**, *28*, 4414–4422.

11. Li, Y.; Xue, Y. Magnetic treatment and its applications to water systems. *Ind. Water Treat.* **2007**, *27*, 11–15.
12. Toussaint, J.F.; Pachot-Clouard, M.; Kantor, H.L. Tissue characterization of atherosclerotic plaque vulnerability by nuclear magnetic resonance. *J. Cardiovasc. Magn. Reson. Off. J. Soc. Cardiovasc. Magn. Reson.* **2000**, *2*, 225–232. [CrossRef] [PubMed]
13. Liu, Z.; Wang, Y.; Gao, Y.; Zhang, L. Synergistic Scale inhibition of polyaspartic acid composite with magnetic field. *Petrochem. Technol.* **2006**, *35*, 891–895. [CrossRef]
14. Song, S.K.; Saksono, N.; Gozan, M.; Bismo, S.; Krisanti, E.; Widaningrum, R. Effects of magnetic field on calcium carbonate precipitation: Ionic and particle mechanisms. *Korean J. Chem. Eng.* **2008**, *25*, 1145–1150.
15. Wang, J.; Li, B.; Liang, Y.; Yin, Z.; Chen, S. Detecting the best electromagnetic field intensity in experiment of electromagnetic anti-fouling based on metastable zone. *CIESC J.* **2016**, *67*, 3658–3662.
16. Deng, A.H.; Huang, H.M.; Ji, W.J. Influence of magnetic field on calcium carbonate precipitation in the presence of foreign ions. *Surf. Eng. Appl. Electrochem.* **2009**, *554–556*, 649–656. [CrossRef]
17. Sun, Y.; Zhu, X.; Han, Y.; Li, Y.; Gao, P. Iron recovery from refractory limonite ore using suspension magnetization roasting: A pilot-scale study. *J. Clean. Prod.* **2020**, *261*, 121221. [CrossRef]
18. Xiao, W.; Zhao, Y.; Yang, J.; Ren, Y.; Yang, W.; Huang, X.; Zhang, L. Effect of sodium oleate on the adsorption morphology and mechanism of nanobubbles on the mica surface. *Langmuir* **2019**, *35*, 9239–9245. [CrossRef]
19. Xiao, W.; Ke, S.; Quan, N.; Zhou, L.; Wang, J.; Zhang, L.; Dong, Y.; Qin, W.; Qiu, G.; Hu, J. The Role of nanobubbles in the precipitation and recovery of organic-phosphine-containing Beneficiation Wastewater. *Langmuir* **2018**, *34*, 6217–6224. [CrossRef]
20. Huang, X.; Zhu, T.; Duan, W.; Liang, S.; Li, G.; Xiao, W. Comparative studies on catalytic mechanisms for natural chalcopyrite-induced Fenton oxidation: Effect of chalcopyrite type. *J. Hazard. Mater.* **2020**, *381*, 120998. [CrossRef]
21. Wang, S.; Hossain, M.Z.; Shinozuka, K.; Shimizu, N.; Kitada, S.; Suzuki, T.; Ichige, R.; Kuwana, A.; Kobayashi, H. Graphene field-effect transistor biosensor for detection of biotin with ultrahigh sensitivity and specificity. *Biosens. Bioelectron.* **2020**, *165*, 112363. [CrossRef] [PubMed]
22. Zhang, S. The relationship between organoclastic sulfate reduction and carbonate precipitation/dissolution in marine sediments. *Mar. Geol.* **2020**, *428*, 106284. [CrossRef]